Plant Molecular Biology (2019) 100:319–333
https://doi.org/10.1007/s11103-019-00862-6

Structural determinants for pyrabactin recognition in ABA receptors in *Oryza sativa*

Seungsu Han[1] · Yeongmok Lee[1] · Eun Joo Park[2] · Myung Ki Min[3] · Yongsang Lee[3] · Tae-Houn Kim[2] · Beom-Gi Kim[3] · Sangho Lee[1]

Received: 4 January 2019 / Accepted: 26 March 2019 / Published online: 2 April 2019

Abstract

Key message **We determined the structure of OsPYL/RCAR3:OsPP2C50 complex with pyrabactin. Our results suggest that a less-conserved phenylalanine of OsPYL/RCAR subfamily I is one of considerations of ABA agonist development for *Oryza sativa*.**

Abstract Pyrabactin is a synthetic chemical mimicking abscisic acid (ABA), a naturally occurring phytohormone orchestrating abiotic stress responses. ABA and pyrabactin share the same pocket in the ABA receptors but pyrabactin modulates ABA signaling differently, exhibiting both agonistic and antagonistic effects. To explore structural determinants of differential functionality of pyrabactin, we determined the crystal structure of OsPYL/RCAR3:pyrabactin:OsPP2C50, the first rice ABA receptor:co-receptor complex structure with a synthetic ABA mimicry. The water-mediated interaction between the wedging Trp-259 of OsPP2C50 and pyrabactin is lost, undermining the structural integrity of the ABA receptor:co-receptor. The loss of the interaction of the wedging tryptophan of OsPP2C with pyrabactin appears to contribute to the weaker functionality of pyrabactin. Pyrabactin in the OsPYL/RCAR3:OsPP2C50 complex adopts a conformation different from that in ABA receptors from *Arabidopsis*. Phe125, specific to the subfamily I of OsPYL/RCARs in the ABA binding pocket, appears to be the culprit for the differential conformation of pyrabactin. Although the gate closure essential for the integrity of ABA receptor:co-receptor is preserved in the presence of pyrabactin, Phe125 apparently restricts accessibility of pyrabactin, leading to decreased affinity for OsPYL/RCAR3 evidenced by phosphatase assay. However, Phe125 does not affect conformation and accessibility of ABA. Yeast two-hybrid, germination and gene transcription analyses in rice also support that pyrabactin imposes a weak effect on the control of ABA signaling. Taken together, our results suggest that phenylalanine substitution of OsPYL/RCARs subfamily I may be one of considerations for ABA synthetic agonist development.

Keywords ABA · Pyrabactin · ABA receptor · Type 2C protein phosphatase · *Oryza sativa*

Introduction

Plants suffer from various inescapable environmental stress due to their immobility. Consequently, sophisticated abiotic stress response mechanisms were developed during its evolutionary history. Abscisic acid (ABA), a phytohormone, plays pivotal roles in seed dormancy, germination, development and responses to abiotic stress such as drought, salinity and

Seungsu Han and Yeongmok Lee have contributed equally.

Accession numbers Diffraction data and coordinates for OsPYL/RCAR3:pyrabactin:OsPP2C50 have been deposited to the protein data bank with the accession number 5ZCU.

Electronic supplementary material The online version of this article (https://doi.org/10.1007/s11103-019-00862-6) contains supplementary material, which is available to authorized users.

✉ Sangho Lee
sangholee@skku.edu

[1] Department of Biological Sciences, Sungkyunkwan University, Suwon 16419, Republic of Korea

[2] Department of Biotechnology, Duksung Women's University, Seoul 01369, Republic of Korea

[3] Gene Engineering Division, Department of Agricultural Biotechnology, National Institute of Agricultural Sciences, Rural Development Administration, Jeonju 55365, Republic of Korea

cold (Cutler et al. 2010; Finkelstein 2013). The core regulatory network in ABA signaling consists of ABA, a soluble ABA receptor PYL/RCAR (pyrabactin resistance/pyrabactin resistance-like/regulatory component of ABA receptor), a co-receptor PP2C (type 2C protein phosphatase), and an effector SnRK2 (sucrose non-fermenting 1-related protein kinase 2) (Fujii et al. 2009; Soon et al. 2012). In normal condition, PP2Cs bind to SnRK2s and inhibit kinase activity of SnRK2s by dephosphorylation of activation loop (Belin et al. 2006; Fujii et al. 2009; Soon et al. 2012). Under abiotic stress, ABA-bound PYL/RCARs compete with SnRK2s for the same binding site of PP2Cs (Soon et al. 2012). Due to their relatively higher affinities, ABA-bound PYL/RCARs bind to PP2Cs, releasing SnRK2s from PP2Cs (Soon et al. 2012). Pyrabactin is a sulfonamide-based synthetic agonist bearing no chemical similarity with ABA, capable of activating some ABA receptors (Park et al. 2009; Zhao et al. 2007). Due to its selective activation of ABA receptors, it was used as a selective agonist for ABA receptor identification (Park et al. 2009). Subsequent studies revealed that selectivity of pyrabactin comes from less-conserved amino acid residues among ABA receptors (Melcher et al. 2010; Peterson et al. 2010; Yuan et al. 2010). Although pyrabactin shows weaker activity than ABA, it shows higher stability and costs less to synthesis than ABA and ABA-related compounds (Cao et al. 2013; Peterson et al. 2010). For this reason, various sulfonamide-based compounds have been developed for agricultural purpose (Cao et al. 2013, 2017; Vaidya et al. 2017).

Oryza sativa harbors ten functional PYL/RCARs excluding constitutively active or deleted forms (He et al. 2014; Kim et al. 2012). OsPYL/RCARs, like AtPYLs of *Arabidopsis*, are classified into three subfamilies based on phylogenetic analysis: monomeric OsPYL/RCAR3, 5, 7 and 8 belong to subfamily I; monomeric OsPYL/RCAR1, 4, and 6 to subfamily II; and dimeric OsPYL/RCAR2, 9 and 10 to subfamily III (Supplementary Fig. S1) (Kim et al. 2012). In *Arabidopsis*, AtPYLs belonging to subfamilies I (AtPYL7, 8, 9 and 10) and II (AtPYL4, 5, 6, 11, 12 and 13) exist as monomers and exhibit strong basal inhibitory effects for PP2Cs in subfamily-dependent manners (Okamoto et al. 2013; Tischer et al. 2017). By contrast, subfamily III members (AtPYR1, AtPYL1, 2 and 3) are dimeric in the absence of ABA, blocking PP2Cs-binding interface and ligand-binding pocket until ABA binding weakens the dimeric interaction (Dupeux et al. 2011b; Zhang et al. 2012). This distinct property of the subfamily III explains its low affinity for ABA and almost no inhibition of PP2Cs without ABA.

Extensive structural and biochemical studies of ABA receptors complexed with ABA and pyrabactin, the representative ABA analog, provide molecular basis for differential affinities between ABA and pyrabactin (Zhang et al. 2015). However, most research on comparative studies of how ABA receptors recognize ABA and pyrabactin at molecular level has been mostly performed in the dicot model plant *Arabidopsis thaliana* (Cao et al. 2013, 2017; Okamoto et al. 2013; Park et al. 2009; Vaidya et al. 2017). In other plants, limited studies have been done about other ABA agonist such as quinabactin and AM1 in tomato (González-Guzmán et al. 2014), bermudagrass (Cheng et al. 2016) and oilseed rape (Naeem et al. 2016; Xiong et al. 2018). However, the structural basis for the differential recognition of ABA and pyrabactin by ABA receptors of the most important monocot crop *Oryza sativa* remains largely unexplored. To uncover the molecular basis for the recognition of pyrabactin by rice ABA receptors, we set out structural and functional characterizations.

Materials and methods

Protein expression and purification

Rosetta 2 (DE3) (Novagen) containing plasmids encoding rice proteins was cultured in LB media containing 1 mM $MgCl_2$ and 0.5% (v/v) glycerol. It was grown at 37 °C until OD_{600} ~ 1.0 for protein overexpression with 0.1 mM IPTG for 5 h at 16 °C with gentle shaking. Harvested cells expressing 6xHis-tagged OsPYL/RCARs were resuspended in buffer A (20 mM Tris–HCl pH 8.0, 200 mM NaCl, 0.5 mM TCEP) with 0.05% (v/v) Triton X-100 and 40 mM imidazole and then lysed by ultrasonication. The cells overexpressing GST-PP2C50 were resuspended in buffer B (20 mM Tris–HCl pH 8.0, 200 mM NaCl, 1 mM $MgCl_2$, 0.5 mM TCEP) with 0.05% (v/v) Triton X-100 and lysed by ultrasonication. The lysates were centrifuged and their supernatants were purified through Ni–NTA agarose resin (Qiagen) for 6×His-tagged OsPYL/RCARs and glutathione-Sepharose 4B resin (GE Healthcare) for GST-tagged OsPP2C50. For next experiments, His-tagged OsPYL/RCARs and GST-tagged OsPP2C50 were dialyzed to the buffer A and the buffer B, respectively.

Protein crystallization

OsPP2C50(58-387) E139A/E140A/K142A was used, which had been introduced previously (Han et al. 2017), to obtain diffraction-quality crystals. To purify OsPP2C50:pyrabactin:OsPYL/RCAR3 complex, bacterial cells expressing 6xHis-tagged OsPP2C50(58-387) E139A/E140A/K142A and OsPYL/RCAR3(30-204) were resuspended together in 40 ml of the buffer B with 0.05% (v/v) Triton X-100, 40 mM imidazole and 0.1 mM pyrabactin (Sigma-Aldrich). After cell lysis and centrifugation of lysate, supernatant was transferred to Ni–NTA resin. Eluate from Ni–NTA resin was treated by recombinant 6xHis-tagged TEV protease to cleave 6×His tag with dialysis to buffer B.

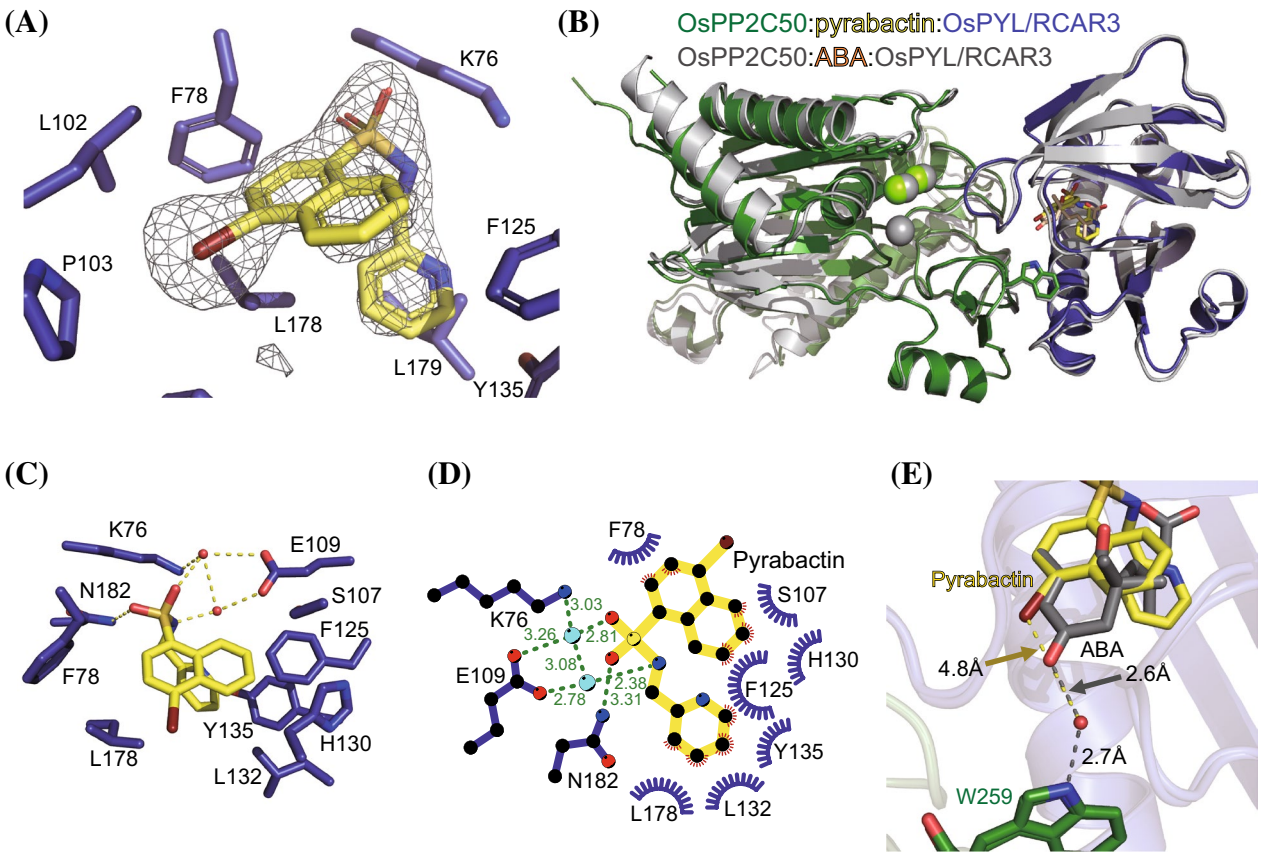

Fig. 1 Structural basis for pyrabactin recognition by ABA receptor/co-receptor complex. **a** 2mFo-DFc omit electron density map of pyrabactin (yellow) and less-conserved two residues (F125 and L178) in OsPYL/RCAR3 (blue):pyrabactin:OsPP2C50 complex (PDB: 5ZCU), contoured at 2.5σ. **b** Overview of OsPP2C50 (green): OsPYL/RCAR3 (blue) complex with pyrabactin (yellow) or ABA (light magenta) (PDB ID 5ZCU and 5GWP, respectively) OsPP2C50 and OsPYL/RCAR3 structures complexed with ABA were colored to gray. **c** Ligand-binding pocket of OsPYL/RCAR3 (blue):OsPP2C50 (green) complex with pyrabactin (yellow). Pyrabactin and ligand-binding residues of ABA receptor/co-receptor complex are represented as stick. **d** Schematic representation of pyrabactin recognition by OsPYL/RCAR3:OsPP2C50 complex. Dashed lines and fan-shaped arcs represent hydrogen-bonds and hydrophobic interactions, respectively. Ligand interaction diagrams are produced by *LigPlot*$^{+}$ (Laskowski and Swindells 2011). **e** ABA (gray), pyrabactin (yellow) and Trp259 (green) of OsPP2C50 are shown in stick model. Dashed gray lines represent water-bridged hydrogen bonds between Trp259 of OsPP2C50 and carbonyl group of ABA. Dashed yellow line represents distance between water and bromine group of pyrabactin

Cleaved 6×-His tag and 6×His-TEV protease were removed through Ni–NTA resin. Furthermore, protein complex was polished by size-exclusion chromatography through HiLoad 16/600 Superdex 200 column (GE HealthCare) in the buffer B with 1 mM TCEP. Finally, the protein complex was concentrated up to 11.8 mg/ml and then the polydispersity of the protein complex was measured by dynamic light scattering on a DynaPro NanoStar (Wyatt) to check probabilities of crystallization. The complex protein crystals were grown at 22 °C in hanging drop, which was performed by mixing 2 µl of the purified complex protein, 1.6 µl of 17% (w/v) PEG3350, 275 mM ammonium sulfate and 0.4 µl of 30% (w/v) sucrose. Crystals appeared within 1–2 days.

Crystallographic data collection and structure determination

We used a single cooled crystal at 100 K in liquid nitrogen gas stream with addition of 20% (w/v) PEG3350 as cryoprotectant. Then, we collected the diffraction data on a Quantum 315r CCD detector (ADSC) on beamline 5C at Pohang Accelerator Laboratory (PAL). Data processing, reduction and scaling were performed by *HKL2000* (Otwinowski and Minor 1997). The complex protein structures of OsPP2C50:pyrabactin:OsPYL/RCAR3 were determined by molecular replacement using *PHASER-MR* of the *PHENIX* suite (Adams et al. 2010) with OsPP2C50:ABA:OsPYL/RCAR3 (PDB ID: 5GWP) (Han et al. 2017) as a search model. *COOT* was used to fit models manually (Emsley and Cowtan 2004), and model refinement was performed

Table 1 Crystallographic date collection and refinement statistics

Crystal	OsPP2C50:pyrabactin:OsPYL/RCAR3
Data collection and processing	
Wavelength (Å)	0.9785
Resolution range (Å)	38.5–2.413 (2.499–2.413)
Space group	$C222_1$
Unit cell (Å) (a, b, c, α, β, γ)	75.04 134.58 190.27 90 90 90
Total reflections	171,385 (16,416)
Unique reflections	36,238 (3202)
Multiplicity	4.7 (4.8)
Completeness (%)	95.91 (86.04)
Mean $I/\sigma(I)$	18.58 (3.68)
Wilson B factor	41.96
R_{merge}	0.0966 (0.5906)
R_{meas}	0.109 (0.6646)
$CC^{1/2}$	0.995 (0.677)
CC^{*}	0.999 (0.899)
Refinement	
R_{work}	0.2075 (0.2548)
R_{free}	0.2510 (0.3245)
CC_{work}	0.941 (0.769)
CC_{free}	0.918 (0.667)
No. of non-hydrogen atoms	7342
Macromolecules	7159
Ligands	58
Water	125
R.m.s.d.	
Bond length	0.005
Bond angle	1.06
Ramachandran plot	
Favored (%)	97.78
Allowed (%)	2.11
Dis-allowed (%)	0.11
Average B factor	
Macromolecules	48.56
Ligands	56.25
Solvent	43.84

Numbers in the highest resolution shell

by *PHENIX* refinement. The data collection and refinement statistics of structures are summarized in Table 1.

Phosphatase activity assay

Phosphatase activity assays were performed in ABA and pyrabactin-dependent manner, following the method as described previously (Han et al. 2017). Briefly, OsPYL/RCAR3, 4, 5, 6, 9 and 10 and OsPP2C50 proteins were prepared following the method with modifications as described previously (Han et al. 2017). 80 nM of GST-PP2C50s and 400 nM of His-OsPYL/RCARs were added in phosphatase assay buffer (20 mM Tris–HCl pH 8.0, 1 mM $MnCl_2$, 0.1% (v/v) 2-mercaptoethanol and 0.1 mg/ml BSA). Various concentrations of ABA and pyrabactin were prepared by serial dilution. Pre-incubation was performed for temperature equilibrium for 20 min at 37 °C. Then, phosphatase activity assay was started by adding 15 mM (final concentration) of pNPP (*p*-nitrophenyl phosphate) as a substrate of the protein phosphatase. After incubation for 1 h at 37 °C, the amount of *p*-nitrophenol was determined by monitoring absorbance at 405 nm. OsPP2C50s' IC_{50} value was calculated by *Prism 5* (GraphPad Software) using the following equation:

$$y = \frac{100}{\left(1 + 10^{(x - \log IC50)}\right)}$$

where x and y refer to relative phosphatase activity (%) and log scale of ABA or pyrabactin concentration (μM), respectively.

Yeast two hybrid assay

Yeast two hybrid assays were conducted using Matchmaker GAL4 two-hybrid system 3 (Clontech). OsPP2Cs were cloned into the prey vector, pGADT7, and OsPYL/RCARs into the bait vector, pGBKT7. Each pair of OsPYL/RCARs and OsPP2Cs was co-transformed into *Saccharomyces cerevisiae* strain AH109 and then plated on synthetic defined minimal (SD) media without leucine and tryptophan (SD-LT) to select transformants. To assay whether pyrabactin can mediate the interaction between OsPP2Cs and OsPYL/RCARs, transformants were transferred to SD-LTH media (SD media without leucine, tryptophan and histidine including 2 mM 3-AT (3-amino-1,2,4-triazole)) supplemented with 0.1, 1, 10, 20 μM ABA or pyrabactin. Pictures for yeast growth were taken 4 days after transfer.

Germination assay

Oryza sativa cg. Dongjin seeds were dehulled and sterilized by following steps; seeds were first sterilized with 70% ethanol for 5 min and then with 50% hydrochloric acid containing 0.5% Tween-20 for 20 min. The seeds were then washed four times in distilled water and once in 70% ethanol. After washing, dehulled seeds were grown under distilled water containing either ABA (10 μM) or pyrabactin (100 μM) for 2, 4, and 7 days ($n = 30$, three biological replicates) and images were taken at each indicated day.

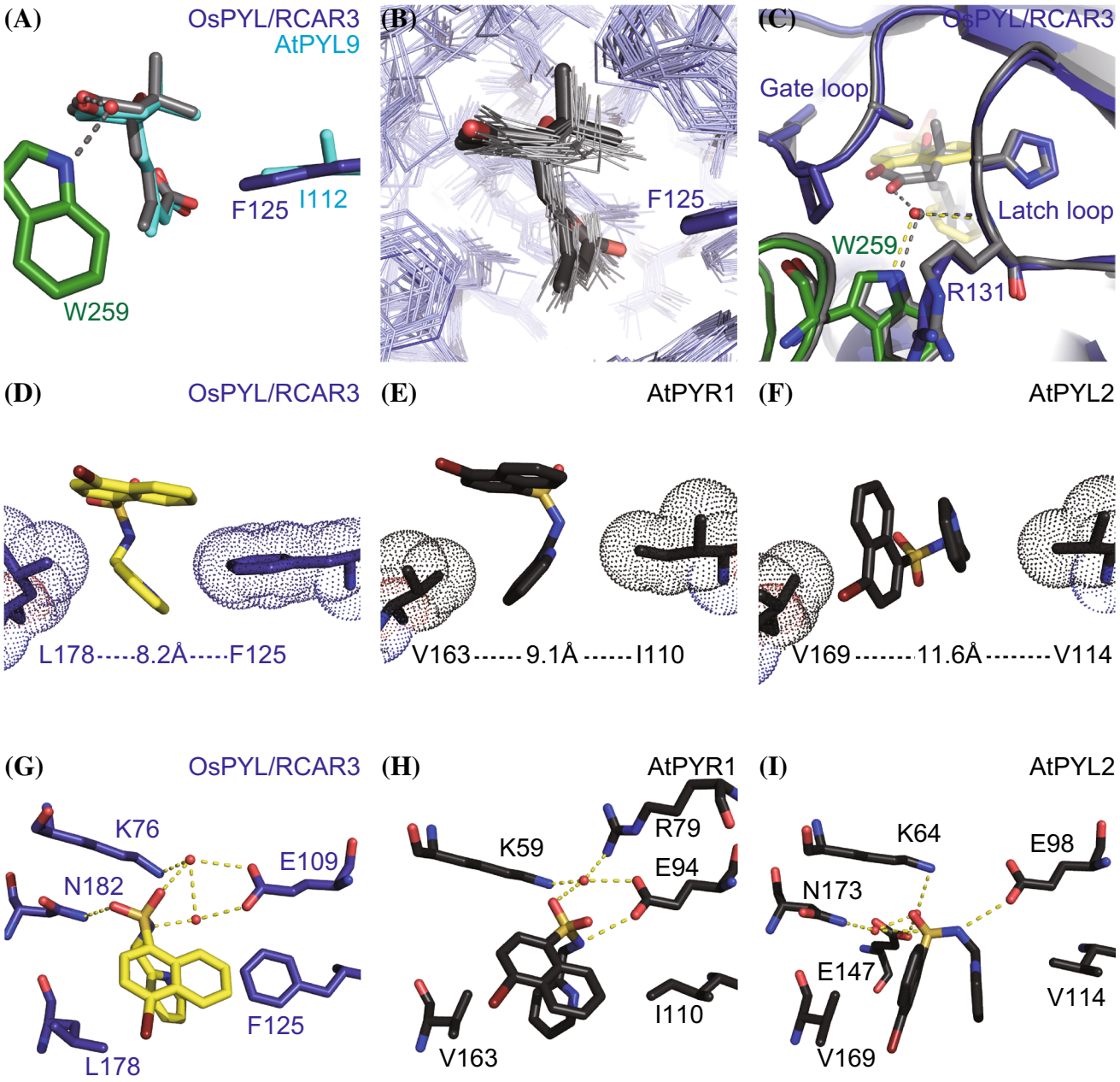

Fig. 2 Comparison of ligand recognition by OsPYL/RCAR3:OsPP2C50 complex and AtPYLs. **a** Superposition of OsPYL/RCAR3:ABA:OsPP2C50 complex (PDB: 5GWP, blue) and (+)-ABA-AtPYL9 (PDB: 3OQU, cyan), which belong to AtPYL subfamily I. Bulky OsPYL/RCAR subfamily I-specific residue (F125, blue, stick) does not clash with ABA. **b** Superpostion of OsPYL/RCAR3:ABA:OsPP2C50 complex (blue, stick and line) and other known ABA-bound ABA receptor structures (light blue, line) (PDB: 3JRQ, 3JRS, 3 K3 K, 3K90, 3KB0, 3KB3, 3KDI, 3QN1, 3R6P, 3UJL, 3W9R, 4DS8, 4DSB, 4DSC, 4OIC, 5JO2, 5MMX, 5MOB, and 5UJV). **c** Superposition of OsPYL/RACR3:pyrabactin:OsPP2C50 complex (PDB: 5ZCU, blue) and OsPYL/RCAR3:ABA:OsPP2C50 complex (gray). Residues of gate and latch loop are represented as stick. **d–f** Front views of OsPYL/RCAR3:pyrabactin:OsPP2C50 (blue), pyrabactin-bound AtPYR1 (PDB: 3NJO, black) and pyrabactin-bound AtPYL2 (PDB: 3NR4, black). In AtPYR1 and AtPYL2, the F125 of OsPYL/RCAR3 was substituted by isoleucine and valine, respectively. **g–i** Top views of OsPYL/RCAR3:pyrabactin:OsPP2C50, pyrabactin-bound AtPYR1 and pyrabactin-bound AtPYL2

RNA isolation and quantitative PCR analysis

Excised radicles from 4-day old seeds were frozen with liquid nitrogen and subsequently pulverized using mortar and pestle. Total RNA was isolated using RNeasy Mini kit (Qiagen). After treatment with DNase I (Takara) for 1 h,

1 µg of total RNA was used for cDNA synthesis (Bioline). The quantitative PCR reaction was performed using SensiFAST™ SYBR® Hi-ROX Kit (Bioline). The internal control for the quantification of gene expressions was *ACT1*. The primers used for quantitative-PCR analyses include, *OsABF1* forward: 5′-TCG CAC ACG GCA TCG GAT CT-3′, reverse: 5′- AGT TGC GTG ACC AGC GAC TC-3′; *OsABI5* forward: 5′-ATG GCA TCG GAG ATG AGC AAG AAC-3′, reverse: 5′-GCT TCT TTG TCA GTA GAA CCG TCT TC-3′; *OsPP2C06* forward: 5′-GAA GAA GTG GGA ACA GGC GT-3′, reverse: 5′-TGC CCG TGA GTC TCC ACA AT-3′; *OsRAB16A* forward: 5′-CAC AGT ACA AAC AAC ACG CAG ACA-3′, reverse: 5′- CCG AGC GCA ATA AAA GGA AA-3′; and *Actin1* forward: 5′-GAT ATG GAG AAG ATC TGG CA-3′, reverse: 5′- TAG CTC TTC TCC ACG GAG GA-3′.

Results

Structural basis for recognition of pyrabactin by OsPYL/RCAR3:OsPP2C50 complex

To understand molecular basis for recognition of pyrabactin by *Oryza sativa* ABA receptors, we performed multiple sequence alignment of ABA receptors from *Oryza sativa* and *Arabidopsis thaliana* (Supplementary Fig. S1). Extensive structural and biochemical characterizations of ABA receptors in *Arabidopsis*, combined with bioinformatics studies, established that key residues involved in ABA and pyrabactin recognition are highly conserved in almost all land plants with only two residues, corresponding to Phe125 and Leu178 of OsPYL/RCAR3, being less conserved (Hauser et al. 2011). With regard to corresponding residues of Leu178 of OsPYL/RCAR3, both OsPYL/RCARs and AtPYLs show three type of substitution, which are leucine, isoleucine and valine, whereas corresponding residues of Phe125 of OsPYL/RCAR3 are only isoleucine and valine, not phenylalanine in AtPYLs (Supplementary Fig. S1). This phenylalaine residue, corresponding to Phe125 of OsPYL/RCAR3, is only found in OsPYL/RCAR subfamily I among ABA receptors in both *Arabidopsis* and *Oryza sativa*. Additionally, OsPYL/RCAR3 represents the highest affinity for pyrabactin among OsPYL/RCARs that we tested in preliminary study (data not shown).

To investigate how rice ABA receptor:co-receptor complex recognize pyrabactin and effects of less-conserved phenylalanine of OsPYL/RCAR3 subfamily I, we solved the crystal structure of OsPYL/RCAR3:pyrabactin:OsPP2C50 complex at 2.45 Å resolution (Fig. 1 and Table 1). To the best of our knowledge, this is the first report of a pyrabactin-bound rice ABA receptor subfamily I structure. Pyrabactin and the less-conserved two residues (Phe125 and Leu178) were well defined in the electron density (Fig. 1a). Overall conformation of the OsPYL/RCAR3:pyrabactin:OsPP2C50 complex is similar to that of the OsPYL/RCAR3:ABA:PP2C50 complex (PDB ID: 5GWP) with pyrabactin essentially occupying the same binding pocket as ABA (Fig. 1b). Pyrabactin recognizing residues mostly overlapping with those recognizing ABA with some differences in OsPYL/RCAR3 (Fig. 1c, d). Many residues are involved in recognizing both ABA and pyrabactin in the same manners. For instance, hydrophobic interactions are mediated by Ser107, Phe125, His130, Leu132, Tyr135, Leu178 of OsPYL/RCAR3, and hydrogen bonds, either direct or water-bridged, are provided by Arg131, Tyr135, Ser137, Glu156, and Asn182 of OsPYL/RCAR3. However, some differences in residues and/or types of interactions are observed for pyrabactin. Phe78, forming a hydrogen bond with ABA, and Val98 recognizes pyrabactin via hydrophobic interactions. Lys76 and Glu109 interact with pyrabactin via water-mediated hydrogen bonds. When we compared conformations of these residues and pyrabactin of two complex molecules in the asymmetric unit, there was no significant difference (r.m.s.d. of 0.185 Å among Cα atoms; Supplementary Fig. S6). Insertion of the conserved wedging tryptophan of PP2Cs to ABA receptor or SnRK2 is reportedly important for binding and water-mediated sensing of the ligand (Dupeux et al. 2011a; Melcher et al. 2009; Soon et al. 2012). Trp259 of OsPP2C50, the conserved wedging tryptophan, interacts differentially with pyrabactin (Fig. 1e). Trp259 forms a water-bridged hydrogen bond with bromine of pyrabactin, similarly to the case of ABA. However, the bromine of pyrabactin is tilted away from the wedging Trp259 compared to carbonyl oxygen of ABA. The bridging water is located further away from the bromine of pyrabactin than that from the carbonyl oxygen of ABA, resulting in much longer (4.8 Å) overall distance than that for ABA (2.6 Å). Such a longer distance between pyrabactin and the bridging water accounts for the lower affinity of pyrabactin to the rice OsPYL/RCAR3:OsPP2C50 complex. The presence of a very weak water-bridged hydrogen bond in the case of pyrabactin is also supported by the observation that only one complex out of two in the asymmetric unit has a water molecule at that position. (Melcher et al. 2009). A previous study reported that proline of the gate loop and arginine of the latch loop also form water-mediated hydrogen bonds with ABA through this water molecule (Melcher et al. 2009). Interestingly, the amide nitrogen of an arginine (R131) in the latch loop instead forms a water-mediated hydrogen bond with the wedging tryptophan (W259) in our structure (Fig. 2c). Taken together, our structural analysis indicates that pyrabactin forms less hydrogen bonds, but similar hydrophobic interactions with OsPYL/RCAR3:OsPP2C50 in comparison with ABA. The less number of overall non-covalent interactions of OsPYL/

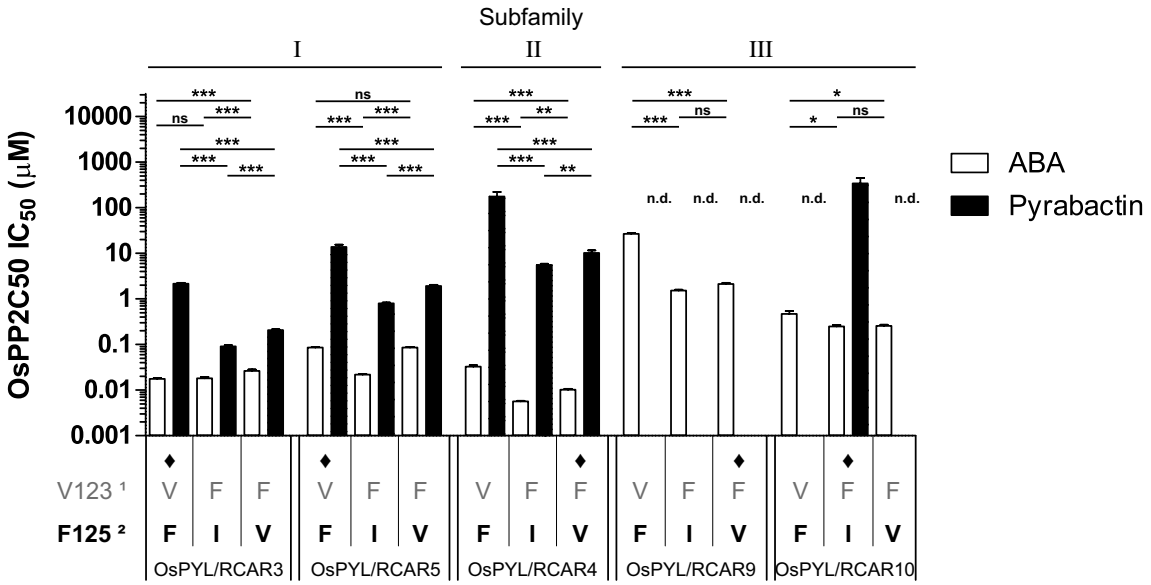

Fig. 3 Inhibition of PP2C by various OsPYL/RCARs and mutants with ABA or pyrabactin. Phosphatase inhibitory effects of OsPYL/RCARs and mutants were measured at different concentartion of ABA or pyrabactin. IC_{50} of ABA or pyrabactin for each OsPYL/RCARs are represented as bar graph. Rows of superscript [1] and [2] indicate residues of each OsPYL/RCARs and mutants, correspond to V123 and F125 of OsPYL/RCAR3. Amino acid pairs of each wild-types are indicated by diamond symbol. The picks depict the average and ± standard error of the mean from triplicates. One-way ANOVA were performed with Tukey's multiple comparison test. *ns* not statistically significant; * p value ≤ 0.05; ** p value ≤ 0.01; *** p value ≤ 0.001; *n.d.,* not determined

RCAR3 and the much weakened water-mediated hydrogen bond between OsPP2C50 with pyrabactin apparently render the OsPYL/RCAR3:OsPP2C50 complex to bind pyrabactin with the weaker affinity than ABA.

OsPYL/RCAR3 recognizes pyrabactin in a slightly different manner than AtPYLs

As the first step to elucidate how OsPYL/RCAR subfamily I-specific phenylalanine residues affect ligand recognition by OsPYL/RCAR3:OsPP2C50 complex, we performed comparative structural analysis of ABA:AtPYL9 (PDB ID: 3OQU), an *Arabidopsis* ABA receptor subfamily I member, and OsPYL/RCAR3:ABA:PP2C50 (PDB ID: 5GWP), the structure we previously reported (Fig. 2a). Distances from AtPYL9 Ile112 to C-3 and C-9 of ABA are 4.9 Å and 3.8 Å, respectively, suggesting that there is ample space to accommodate substitution of phenylalanine, a bulky hydrophobic residue, for isoleucine. Distances from OsPYL/RCAR3 Phe125 to C-3 and C-9 of ABA are 4.0 Å and 3.6 Å, featuring reduced distances. However, this reduction in distance to ABA does not seem to be sufficient for causing van der Waals repulsion. Rotameric differences were observed in AtPYL9 Ser94 and Ser124 and OsPYL/RCAR3 Ser107 and Ser137 with no influence on the position of the ligand, ABA, and its binding. Overall, no significant conformational difference in the ligand binding pocket was observed between AtPYL9 and OsPYL/RCAR3 (Fig. 2a and Supplementary Fig. S2). Superposition of the structure of ABA-bound OsPYL/RCAR3 with those of other known ABA-bound ABA receptors confirmed no significant difference in the local conformation of the ligand binding pocket (Fig. 2b). In the OsPYL/RACR3:pyrabactin:OsPP2C50 structure, pyrabactin occupies the agonistic position that ABA assumes and also induces proper gate loop closure as ABA-bound structure (Fig. 2c).

We performed structural comparison of pyrabactin-bound OsPYL/RCAR3 with known pyrabactin-bound *Arabidopsis* orthologs to investigate differential molecular determinants in recognition of pyrabactin by OsPYL/RCAR3 (Fig. 2d–i). We focused on the effects of two less conserved residues in the ligand binding pocket of OsPYL/RCAR3 on the recognition of pyrabactin: Phe125 in β5 and Leu178 in α4 (Supplementary Fig. S1). These two residues pack pyridine moiety of pyrabactin from opposite sides by hydrophobic interactions (Fig. 2d and Supplementary Fig. S3a). Residues in these positions are less conserved and known to be critical in determining whether pyrabactin triggers gate loop closure of ABA receptors, evidenced by structural analyses of pyrabactin-bound AtPYR1 and AtPYL1-3 (Melcher et al. 2010; Peterson et al. 2010; Yuan et al. 2010; Zhang et al. 2012, 2015). Distance between the less conserved hydrophobic residues in the ligand binding pocket of ABA receptors appears to be a major culprit for conformational differences of pyrabactin (Fig. 2d, e, f). OsPYL/RCAR3 Phe125 corresponds to AtPYR1 Ile110 and AtPYL2 Val114.

Pairing of Phe125 with Leu178 of OsPYL/RCAR3 and that of Ile110 with Val163 of AtPYR1 result in distances being 8.2 and 9.1 Å, respectively, with pyrabactin occupying the same position as ABA, thereby rendering pyrabactin to act as an agonist (Fig. 2e and Supplementary Fig. S3b). By contrast, pairing of AtPYL2 Val114 with Val169 makes the corresponding distance 11.6 Å with pyrabactin assuming an antagonist position (Fig. 2f and Supplementary Fig. S3c). When comparing the pairing residues in AtPYR1 and AtPYL2, only difference is the identity of the residue corresponding to OsPYL/RCAR3 Phe125. Valine is simply one carbon shorter than isoleucine, but this small change permits pyrabactin to rotate about 90 degrees in the ligand binding pocket of AtPYL2 and 3 (Yuan et al. 2010). Such conformational change of pyrabactin in AtPYL2 and 3 allows its bromonaphtalene group to face AtPYL2 Val169 (AtPYL3 Val192), and pyridine group of pyrabactin AtPYL2 Val114 (AtPYL3 Val134) (Fig. 2f and Supplementary Fig. S3c). Bromine atom of bromonaphtalene group of pyrabactin mimics the carbonyl group of ABA. The buried bromine atom caused by rotation of pyrabactin is incapable of closing the gate loop and generating the water-mediated interaction between pyrabactin and co-receptor PP2C (Miyakawa et al. 2013; Peterson et al. 2010; Yuan et al. 2010). Our comparative structural analysis revealed that previously unreported bulky Phe125 of OsPYL/RCAR3 also permits pyrabactin-induced gate loop closure, yet phenylalanine makes conformational differences in pyrabactin recognition by narrowing the ligand binding pocket, compared with isoleucine or valine.

In addition to differential microenvironment in positioning the pyridine moiety, microenvironment around sulfonamide moiety of pyrabactin undergoes subtle changes (Fig. 2g, h, i). For instance, distances from Cγ atom of OsPYL/RCAR3 Phe125 to atoms of the sulfonamide moiety increase by 2.4 Å (sulfur) to 2.9 Å (nitrogen), compared to those from Cγ1 atom of AtPYR1 Ile110 (Fig. 2g vs. h). Such a shift of the sulfonamide group induces rearrangement of hydrogen bonding network in the ligand binding pocket. In AtPYR1 and AtPYL1, the sulfonamide moiety of pyrabactin mimics a water molecule mediating a hydrogen bond between AtPYR1 Glu94 (AtPYL1 Glu98) and the hydroxyl group of ABA (Yuan et al. 2010). AtPYR1 Glu94 (AtPYL1 Glu100) and AtPYR1 Lys59 (AtPYL1 Lys65) interact with pyrabactin via a direct hydrogen bond between AtPYR1 Glu94 and nitrogen of the sulfonamide group and a water-mediated hydrogen bond between AtPYR1 Glu94 and Lys59 and a sulfonyl oxygen (Fig. 2h). In OsPYL/RCAR3, hydrogen bonding network centered on the sulfonamide group is slightly tweaked presumably due to the relative shift of the sulfonamide group. Notably, the direct hydrogen bond between AtPYR1 Glu94 (AtPYL2 Glu98) and the nitrogen of the sulfonamide group is replaced by a water-mediated one between OsPYL/RCAR3 Glu109 and the nitrogen (Fig. 2g–i).

Functional consequences of pyrabactin binding to OsPYL/RCAR:OsPP2C complexes

To probe interactions between OsPYL/RCARs representing all three subfamilies and OsPP2C50, we performed phosphatase activity assay with ABA or pyrabactin added at varying concentrations (Fig. 3 and Supplementary Fig. S4). A low half-maximal inhibitory concentration (IC_{50}) indicates high affinity between OsPYL/RCARs and OsPP2C50. Consistent with previous reports, all five OsPYL/RCARs (OsPYL/RCAR3 and 5 in subfamily I, OsPYL/RCAR4 in subfamily II, and OsPYL/RCAR9 and 10 in subfamily III) exhibited lower affinities towards pyrabactin than ABA. Notably, OsPYL/RCARs in subfamily III showed weaker affinities towards both pyrabactin and ABA and the difference in affinities for a given OsPYL/RCAR appears to be less severe. Such observations are in line with reports for AtPYLs (Miyakawa et al. 2013), reflecting the dimeric state of the ABA receptors in the subfamily III.

To investigate how OsPYL/RCAR3 Phe125 substitution affects binding affinity with OsPP2C50, we attempted to produce OsPYL/RCAR3 F125I and F125V mutants in *E. coli* without success (data not shown). Careful examination of multiple sequence alignment on the positions of OsPYL/RCAR3 Val123 and Phe125 revealed that these two positions often have complementary hydrophobic residues identities: pairing of an aliphatic residue such as valine and isoleucine with aromatic phenylalanine, implicating that such a pairing may be important for structural integrity. For instance, AtPYL13, an ABA-irresponsive receptor with both positions occupied by aliphatic valine and isoleucine, was not expressed alone in *E. coli* with unknown reasons (Li et al. 2013). We subsequently prepared double mutants OsPYL/RCAR3 V123F/F125I and V123F/F125V. These double mutants were successfully expressed in *E. coli*. Since Val123 is not an ABA- or pyrabactin-binding residue, we reasoned that the mutation of Val123 might not affect ligand binding. In addition, all wild-type OsPYL/RCARs have one of these three types of pair: VF, FI and FV (Supplementary Fig. S1) where the first letter indicates corresponding residue of Val123 of OsPYL/RCAR3 and the latter one is corresponding residue of Phe125 of OsPYL/RCAR3. For these reasons, we also prepared other four OsPYL/RCARs mutants in the same manner, excluding OsPYL/RCAR6 due to its low expression level.

ABA binding of OsPYL/RCAR3 double mutants showed no noticeable difference compared to that of wild-type (WT): IC_{50} values are 17.7 nM for WT, 18.4 nM for V123F/F125I and 26.4 nM for V123F/F125V (Fig. 3). However, pyrabactin

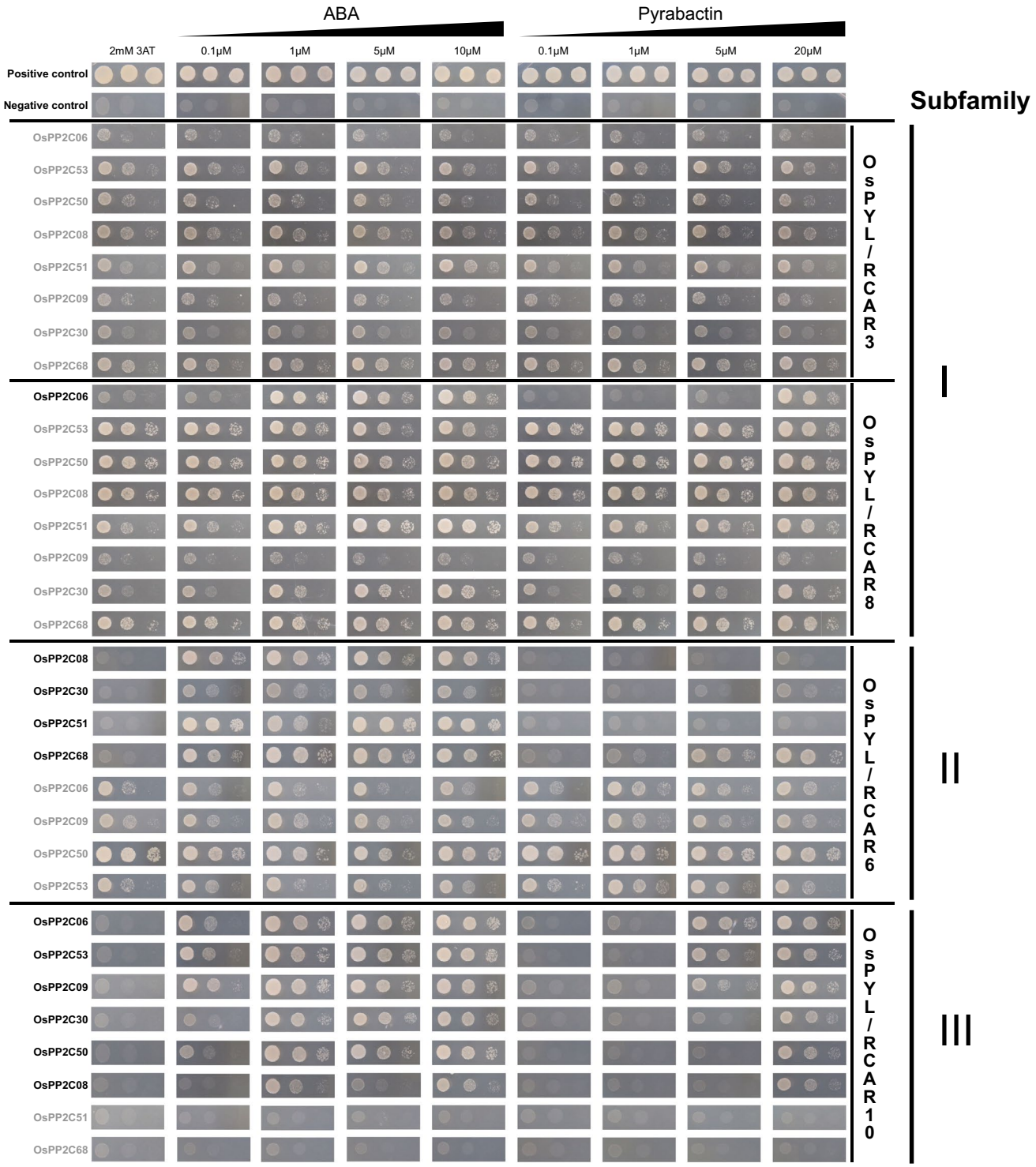

Fig. 4 Survey of the interactions between selected OsPYL/RCARs and OsPP2Cs by yeast two hybrid assay. OsPYL/RCAR3, 8 (subfamily I), 6 (subfamily II), and 10 (subfamily III) were subject to interact with OsPP2C06, 08, 09, 30, 50, 51, 53, and 68. Four different concentrations of ABA and pyrabactin were added to selection media. Black-colored PP2Cs mean ABA- or pyrabactin-dependent interaction with ABA receptor and gray-colored PP2Cs mean ABA- and pyrabactin-independent interaction or non-interaction by both ligand in the yeast two hybrid assay

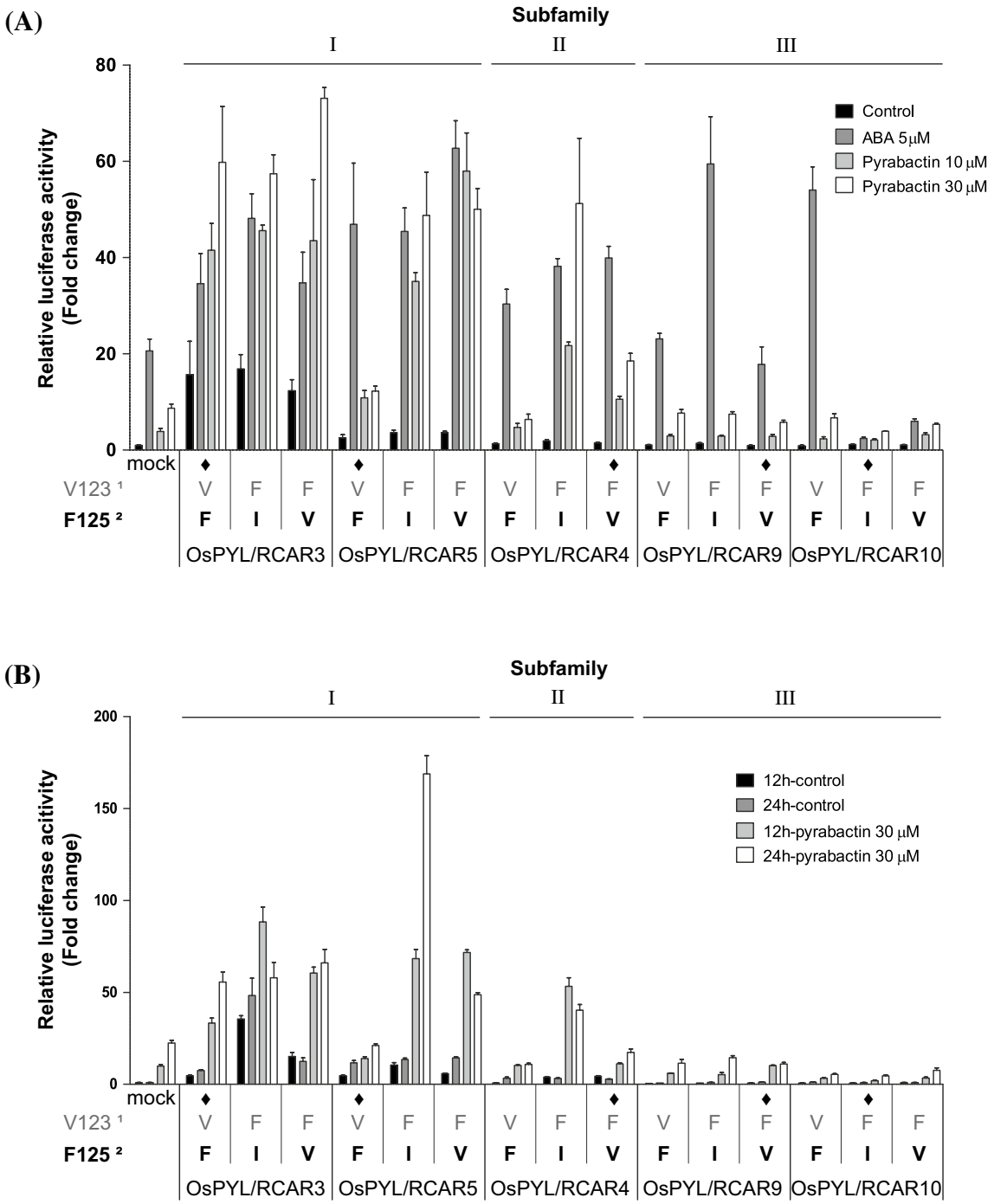

Fig. 5 Induction of ABA signaling by OsPYL/RCARs and mutants with ABA or pyrabactin. Transient overexpression of OsPYL/RCARs wild-type and mutants was performed in rice protoplasts. Ligand-induced ABA signaling activations were evaluated by a dual-luciferase reporter assay with an ABA-inducible promoter. Rows of superscript 1 and 2 indicate residues of each OsPYL/RCAR and its mutant, corresponding to Val123 and Phe125 of OsPYL/RCAR3, respectively. Amino acid residue pairs of each wild-type are indicated by diamond symbol. **a** ABA or pyrabactin was treated with different concentrations. Luciferase activities were measured at 18 h after treatment with either ABA or pyrabactin. The resulting luciferase activities were normalized to mock control. **b** Time-dependent ABA-signaling activations were measured at 12 h and 24 h after 30 μM pyrabactin treatment. The resulting luciferase activities were normalized to 12 h mock control. The picks depict the average and ± standard deviation from triplicates

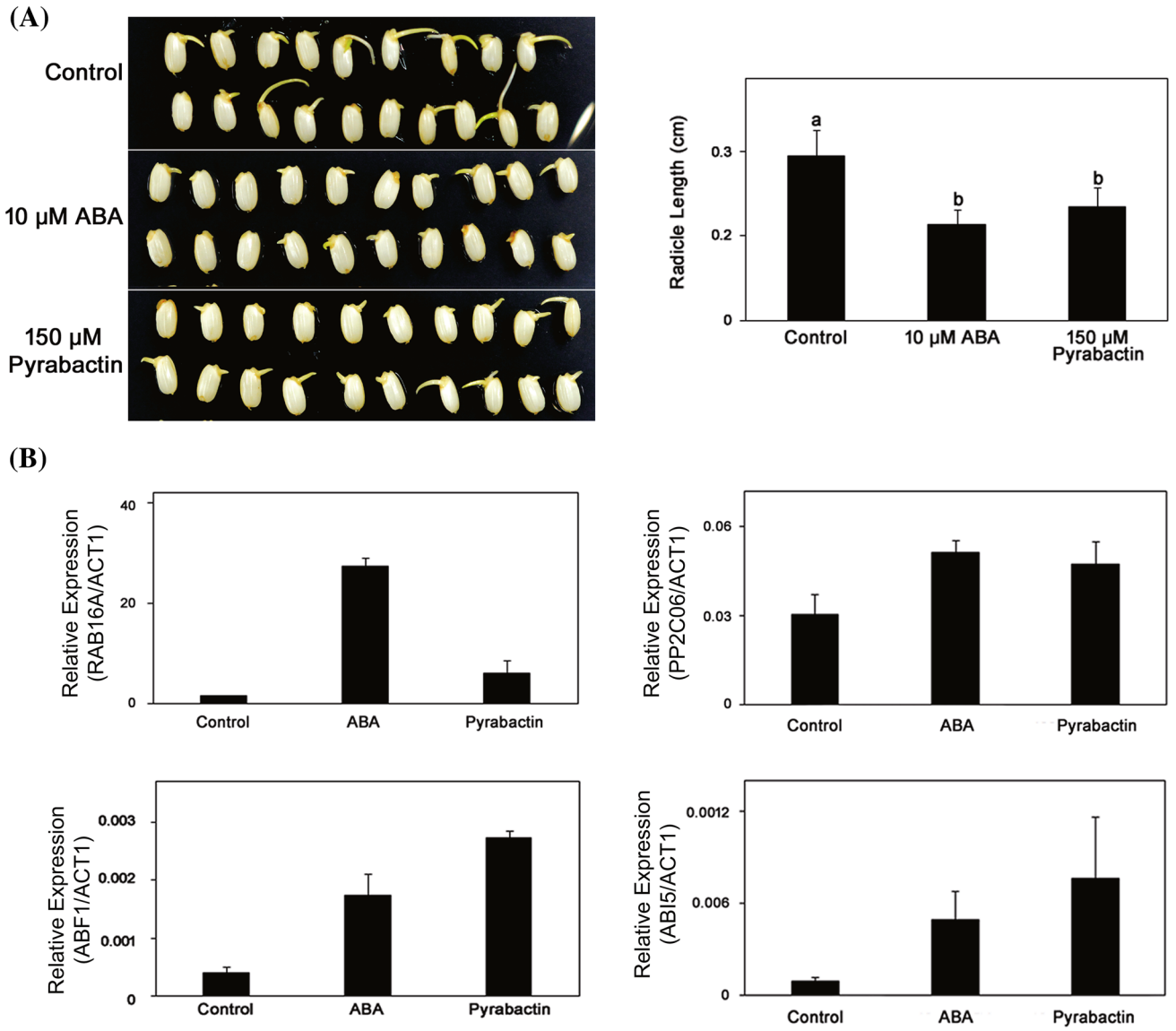

Fig. 6 Pyrabactin produced ABA effects at germination and early post germination stages in rice. **a** Dehulled *Oryza sativa cv. Dongjin* seeds were grown under distilled water containing either ABA (10 μM) or pyrabactin (150 μM) for 3 days ($n = 19$, four biological replicates), and then radicle length was measured using *Image J* (Schneider et al. 2012). The letters "a" and "b" indicate different group based on one way ANOVA, Tukey's post hoc test, p value < 0.05. **b** The relative gene expressions of *RAB16A, PP2C06, ABI5*, and *ABF1* were measured by quantitative PCR using *ACT1* as an internal control. Total RNA was isolated from 4-day old seed radicles germinated under ABA (10 μM) or pyrabactin (100 μM) treatment ($n = 7$, three biological replicates). The picks depict the average and ± standard error of the mean

binding of the double mutants showed clear differences in their affinities: IC_{50} values are 2160 nM for WT, 91.6 nM for V123F/F125I and 206 nM for V123F/F125V. Substitution of Phe125 for both isoleucine and valine resulted in significant increases in affinities toward pyrabactin: ~ 24-fold increase for isoleucine and ~ tenfold increase for valine in comparison for WT. Consistently, all other OsPYL/RCARs of subfamily I and II (OsPYL/RCAR5 and 4) showed similar detrimental effects of phenylalanine substitution toward pyrabactin in comparison to either valine or isoluecine: Phenylalanine showed the weakest affinity while isoleucine showed slightly stronger affinity than valine. Similar residue-specific affinity changes were observed in ABA binding: most isoleucine mutants showed stronger affinity to ABA than other mutants, whereas valine or phenylalanine mutants lower affinity. We were unable to determine IC_{50} values of OsPYL/RCAR9 and OsPYL/RCAR10 of subfamily III due to low affinity toward pyrabactin, except for OsPYL/RCAR10 WT. Phenylalanine substitution in the subfamily III OsPYL/RCARs also showed the weakest affinity toward ABA. Previous

reports showed that isoleucine or valine in the position of Phe125 of OsPYL/RCAR3 determines whether pyrabactin occupies as agonistic or antagonistic position in AtPYLs (Peterson et al. 2010; Yuan et al. 2010). Our results revealed that difference in the affinity for pyrabactin between isoleucine and valine substitution was modest. These confliction may be derived from different subfamily or species-specific features of ABA receptors. Previous reports about pyrabactin only refer ABA receptor subfamily III in *Arabidopsis thaliana* (Peterson et al. 2010; Yuan et al. 2010), but our data also provide pyrabactin recognition of subfamily I and II in *Oryza sativa*. Nevertheless, these results reinforce the idea that narrow pyrabactin binding cleft caused by bulky phenylalanine may affect accessibility of pyrabactin. Collectively, our phosphatase assay results support structural analysis that the presence of the less conserved Phe125 in the ligand binding pocket contributes to weakening the pyrabactin binding by OsPYL/RCAR3 and subfamily I paralogs.

Pyrabactin mediates interactions between OsPYL/RCARs and clade A PP2Cs differentially

Our structural and biochemical characterizations of pyrabactin recognition by OsPYL/RCAR:OsPP2C complexes suggested differential pyrabactin recognition depending on specific OsPYL/RCAR:OsPP2C pairing. To investigate how pyrabactin mediates interactions between OsPYL/RCARs and clade A PP2Cs in rice, we performed yeast two hybrid experiments using eight clade A PP2Cs (OsPP2C06, 08, 09, 30, 50, 51, 53, and 68) and four ABA receptors representing three subfamilies (OsPYL/RCAR3, 6, 8 and 10) using selection media supplemented with either ABA or pyrabactin at varying concentrations (Fig. 4). OsPYL/RCAR3 and 8 belong to the subfamily I, OsPYL/RCAR6 to the subfamily II and OsPYL/RCAR10 to the subfamily III. OsPYL/RCAR3 showed concentration-independent interactions with all the tested OsPP2Cs for both ABA and pyrabactin, in some accordance with the phosphatase activity assay results despite details being different. OsPYL/RCAR8, a member of subfamily I, exhibited a concentration-dependent interaction with OsPP2C06 for both ABA and pyrabactin with the interaction being more sensitive to ABA. Such differential interactions mediated by ABA and pyrabactin were also observed for OsPYL/RCAR6, a member of subfamily II. OsPYL/RCAR6 interacted with OsPP2C08, 30, 38 and 51 in ABA-dependent manners while the pyrabactin-dependent interaction was observed only between OsPYL/RCAR6 and OsPP2C68. OsPYL/RCAR10, a member of subfamily III, required at least 0.1 μM ABA to interact with OsPP2Cs except for OsPP2C51 and 68, indicating reduced ABA sensitivity in comparison to subfamily I and II members. Pyrabactin also mediated the interactions between OsPYL/RCAR10 and OsPP2Cs similarly to those mediated by ABA, but required a higher concentration (at least 5 μM) than ABA. Some OsPPC2s such as OsPP2C06 or OsPPC2C53 showed better affinity to pyrabactin with OsPYL/RCAR10 than OsPP2C50 of our phosphatase activity assay. These data suggest that each OsPYL/RCAR and OsPP2C interaction pair reacts differentially to pyrabactin as well as ABA.

Pyrabactin recognition of OsPYL/RCARs and mutants affects ABA signaling activation

To determine comprehensive effects of OsPYL/RCARs and mutants on ABA signaling pathway by pyrabactin *in planta*, we conducted luciferase assay in rice protoplasts with ABA and pyrabactin treatments (Fig. 5). We used the same OsPYL/RCARs and their double mutants used in the phosphatase activity assay. Interestingly, the extents of ABA signaling activation by either ABA or pyrabactin are different depending on the ABA receptor subfamily (Fig. 5a). OsPYL/RCARs of subfamilies I and II showed similar responses to ABA regardless of mutations, but different responses to pyrabactin each double mutant. OsPYL/RCAR3 WT and double mutants showed high basal activity in the absence of either ABA or pyrabactin. It is consistent with the yeast two hybrid results, which showed either ABA or pyrabactin-independent interaction of OsPYL/RCAR3 WT. Notably, they exhibited activation by pyrabactin in a concentration-dependent manner. Isoleucine substitution in OsPYL/RCAR3 made its response to pyrabactin worse than to ABA in comparison to WT, consistent with the phosphatase activity assay result. Isoleucine or valine substitution in OsPYL/RCAR5 and 4 showed increased signaling activation by pyrabactin than WT. Taken together, phenylalanine, isoleucine and valine substitutions of OsPYL/RCARs belonging to subfamilies I and II mainly affect pyrabactin-induced activation, not ABA-induced one. In contrast, OsPYL/RCAR9 and 10 belonging to subfamily III represented poor activation by pyrabactin. However, isoleucine substitution in OsPYL/RCAR9 and phenylalanine substitution in OsPYL/RCAR10 showed significant activation by ABA. We also investigated changes in activation of ABA signaling by pyrabactin at different time points (Fig. 5b). Subfamily I OsPYL/RCARs exhibited most notable activation increases in time-dependent manners with subfamily II OsPYL/RCAR4 featuring less pronounced activation increase. By contrast, no significant activation increase was observed in subfamily III OsPYL/RCARs. Collectively, these results imply that these three types of substitution in OsPYL/RCARs can affect ABA signaling pathway *in planta*. OsPYL/RCARs of subfamilies I and II mainly mediate pyrabactin-induced responses, and phenylalanine residue in subfamily I OsPYL/RCARs may interfere ABA signaling activation by pyrabactin.

Pyrabactin induce ABA response during seed germination in *Oryza sativa*

Physiological effects of pyrabactin in rice has not been reported thus far. To examine effects of pyrabactin on the ABA signaling in rice, we conducted germination assays using dehulled *Oryza sativa cv. Dongjin* seeds in the presence of 10 μM ABA or 150 μM pyrabactin (Fig. 6a). Compared to control, seed germination and post-germination development of rice were inhibited in response to pyrabactin. Requirement of higher concentration of pyrabactin to see the similar level of germination inhibition than that of ABA is consistent to the structural and biochemical data showing weak interactions of OsPYL/RCARs:OsPP2Cs with pyrabactin compared to ABA (Figs. 2c, 3).

Recognition of pyrabactin by OsPYL/RCARs prompted us to reason that pyrabactin might induce stress responses in rice as shown in Arabidopsis (Park et al. 2009). To investigate the effect of pyrabactin on the induction of ABA-regulated stress-responsive gene expression in rice, we performed quantitative PCR by using total RNAs of 4-day old seed radicles. Although we observed overall induction of the rice stress-responsive genes in response to pyrabactin, the induced levels of each genes by pyrabactin varied compared to the ABA treatment. The induction of *RESPONSIVE TO ABSCISIC ACID 16A* (*RAB16A*) by pyrabactin was lower than by ABA, suggesting that weaker interactions of OsPYL/RCARs and OsPP2Cs with pyrabactin than those with ABA lead to incomplete inhibition of OsPP2Cs activity (Fig. 6b). However, the pyrabactin induction of *PROTEIN PHOSPHATASE 2C 06* (*PP2C06*), *ABSCISIC ACID RESPONSE ELEMENT BINDING FACTOR 1* (*ABF1*), and *ABSCISIC ACID-INSENSITIVE 5* (*ABI5*) gene expressions were similar or even higher than the ABA treatment (Fig. 6b). These differential gene expression patterns might have been produced by the pyrabactin-dependent activation of certain ABA perception pathways from the full set of ABA receptors. In line with this observation, another ABA agonist quinabactin was shown to specifically induce a certain set of stress-responsive genes depending on the tested species such as soybean or barley (Okamoto et al. 2013). Furthermore, recent transcriptome analysis study in *Brassica napus* showed that a sulfonamide-based ABA agonist ABA mimics 1 (AM1) exhibits similar effects under drought stress (Xiong et al. 2018). Both ABA and AM1 treatment showed similar transcriptomal changes in *Brassica napus*. However, in detail, some genes showed different changes of gene expression level. Taken together, these results demonstrate that pyrabactin has some physiological effects in rice and can cause stress-responsive rice gene expressions with some differences from ABA treatment.

Discussion

ABA receptors feature the highly conserved ligand binding pocket with small number of residue variations (Hauser et al. 2011). A change in these varying residues such as isoleucine and valine, corresponding to Phe125 in OsPYL/RCAR3, reportedly leads to different pyrabactin sensitivity among AtPYLs (Melcher et al. 2010; Peterson et al. 2010; Yuan et al. 2010). This variation of isoleucine or valine in the ligand binding pocket determines selectivity of ABA receptors toward phaseic acid, a metabolite of ABA, resulting in sophisticated modulation of ABA response (Weng et al. 2016). These studies demonstrate that different ligand sensitivities of *Arabidopsis* ABA receptors can be derived from small difference in specific residues such as isoleucine to valine in the ligand binding pocket. In this study, we revealed how the less conserved OsPYL/RCAR3 Phe125 modulates recognition of pyrabactin differently from those of other pyrabactin-bound ABA receptors by combination of structural and biochemical techniques. OsPYL/RCAR3 Phe125, corresponding to AtPYR1 Ile110 and AtPYL2 Val114, clashes with the known conformations of pyrabactin. Pyrabactin in our OsPYL/RCAR3:OsPP2C50 structure represents a different conformation featuring twist of pyridine group and altered hydrogen bonding network caused by shift of sulfonamide group in comparison to the reported pyrabactin conformations. Despite its different conformation, pyrabactin in OsPYL/RCAR3 assumes the agonist position evidenced by the same closed conformation of gate loop as that found in other *Arabidopsis* ABA receptors (Fig. 2c) (Melcher et al. 2009). The presence of Phe125 apparently creates a narrow cavity restricting access of pyrabactin, supported by increased affinities when Phe125 was mutated to either isoleucine or valine. OsPYL/RCAR3 Phe125 is conserved among subfamily I members of rice ABA receptors (Supplementary Fig. S1). Our structural work provide the first glimpse on the role of Phe125 in the subfamily I of ABA receptors in general as well as in pyrabactin recognition by rice ABA receptors. It is noteworthy that Phe125 is apparently complementary to Val123 in OsPYL/RCAR3 to ensure structural integrity. Such complementary combination is observed in some members of subfamily II and all members of subfamily III among rice and *Arabidopsis* ABA receptors (Supplementary Fig. S1). OsPYL/RCAR3 Phe125 is also found in many monocots including *Zea mays* (maize), *Zoysia japonica* (lawngrass), *Brachypodium distachyon* (stiff brome), *Phoenix dactylifera* (date palm), *Setaria italic* (foxtail millet), and some dicots such as *Coffea canephora* (robusta coffee). Our structural and functional results for phenylalanine substitution for isoleucine or valine in *Arabidopsis*, would contribute to developing more effective ABA synthetic agonists for many plants and crops.

Acknowledgements We thank the staff members at beamline 5C, Pohang Accelerator Laboratory for technical assistance in crystallographic data collection. This work was supported by the Next-Generation BioGreen 21 Program (PJ01335001 and PJ01367602) through the Rural Development Agency and the National Research Foundation of Korea grants awarded by the Basic Science Research Program (NRF-2018R1A2B6004367) and the Science Research Center Program (SRC-2017R1A5A1014560).

Author's contributions SL conceived research plans and supervised experiments. SH and SL designed experiments. SH and YL performed most of the experiments and analyzed the data. EJP, MKM, YL, T-HK, and B-GK performed some experiments and analyzed the data for supporting main idea. SH, YL, and SL wrote the article with contributions of all the authors.

Data availability The datasets generated during and/or analysed during the current study such as diffraction data and coordinates for OsPYL/RCAR3:pyrabactin:OsPP2C50 are available in the protein data bank repository with the accession number 5ZCU at http://www.rcsb.org/structure/5ZCU.

References

Adams PD et al (2010) PHENIX: a comprehensive Python-based system for macromolecular structure solution. Acta Crystallogr D 66:213–221. https://doi.org/10.1107/s0907444909052925

Belin C et al (2006) Identification of features regulating OST1 kinase activity and OST1 function in guard cells. Plant Physiol 141:1316–1327. https://doi.org/10.1104/pp.106.079327

Cao M et al (2013) An ABA-mimicking ligand that reduces water loss and promotes drought resistance in plants. Cell Res 23:1043–1054. https://doi.org/10.1038/cr.2013.95

Cao MJ et al (2017) Combining chemical and genetic approaches to increase drought resistance in plants. Nat Commun 8:1183. https://doi.org/10.1038/s41467-017-01239-3

Cheng Z, Jin R, Cao M, Liu X, Chan Z (2016) Exogenous application of ABA mimic 1 (AM1) improves cold stress tolerance in bermudagrass (*Cynodon dactylon*). Plant Cell Tissue Organ Cult (PCTOC) 125:231–240. https://doi.org/10.1007/s11240-016-0941-5

Cutler SR, Rodriguez PL, Finkelstein RR, Abrams SR (2010) Abscisic acid: emergence of a core signaling network. Annu Rev Plant Biol 61:651–679. https://doi.org/10.1146/annurev-arplant-042809-112122

Dupeux F et al (2011a) Modulation of abscisic acid signaling in vivo by an engineered receptor-insensitive protein phosphatase type 2C allele. Plant Physiol 156:106–116. https://doi.org/10.1104/pp.110.170894

Dupeux F et al (2011b) A thermodynamic switch modulates abscisic acid receptor sensitivity. EMBO J 30:4171–4184. https://doi.org/10.1038/emboj.2011.294

Emsley P, Cowtan K (2004) Coot: model-building tools for molecular graphics. Acta Crystallogr D Biol Crystallogr 60:2126–2132. https://doi.org/10.1107/s0907444904019158

Finkelstein R (2013) Abscisic acid synthesis and response. Arabidopsis Book 11:e0166. https://doi.org/10.1199/tab.0166

Fujii H et al (2009) vitro reconstitution of an abscisic acid signalling pathway. Nature 462:660–664. https://doi.org/10.1038/nature08599

González-Guzmán M et al (2014) Tomato PYR/PYL/RCAR abscisic acid receptors show high expression in root, differential sensitivity to the abscisic acid agonist quinabactin, and the capability to enhance plant drought resistance. J Exp Bot 65:4451–4464. https://doi.org/10.1093/jxb/eru219

Han S et al (2017) Modulation of ABA signaling by altering VxG-PhiL motif of PP2Cs in *Oryza sativa*. Mol Plant 10:1190–1205. https://doi.org/10.1016/j.molp.2017.08.003

Hauser F, Waadt R, Schroeder JI (2011) Evolution of abscisic acid synthesis and signaling mechanisms. Curr Biol CB 21:R346–R355. https://doi.org/10.1016/j.cub.2011.03.015

He Y, Hao Q, Li W, Yan C, Yan N, Yin P (2014) Identification and characterization of ABA receptors in *Oryza sativa*. PLOS ONE 9:e95246. https://doi.org/10.1371/journal.pone.0095246

Kim H et al (2012) A rice orthologue of the ABA receptor, OsPYL/RCAR5, is a positive regulator of the ABA signal transduction pathway in seed germination and early seedling growth. J Exp Bot 63:1013–1024. https://doi.org/10.1093/jxb/err338

Laskowski RA, Swindells MB (2011) LigPlot+: multiple ligand–protein interaction diagrams for drug discovery. J Chem Inf Model 51:2778–2786. https://doi.org/10.1021/ci200227u

Li W et al (2013) Molecular basis for the selective and ABA-independent inhibition of PP2CA by PYL13. Cell Res 23:1369–1379. https://doi.org/10.1038/cr.2013.143

Melcher K et al (2009) A gate-latch-lock mechanism for hormone signalling by abscisic acid receptors. Nature 462:602–608. https://doi.org/10.1038/nature08613

Melcher K et al (2010) Identification and mechanism of ABA receptor antagonism. Nat Struct Mol Biol 17:1102–1108. https://doi.org/10.1038/nsmb.1887

Miyakawa T, Fujita Y, Yamaguchi-Shinozaki K, Tanokura M (2013) Structure and function of abscisic acid receptors. Trends Plant Sci 18:259–266. https://doi.org/10.1016/j.tplants.2012.11.002

Naeem MS, Dai L, Ahmad F, Ahmad A, Li J, Zhang C (2016) AM1 is a potential ABA substitute for drought tolerance as revealed by physiological and ultra-structural responses of oilseed rape. Acta Physiol Plant 38:183. https://doi.org/10.1007/s11738-016-2190-y

Okamoto M et al (2013) Activation of dimeric ABA receptors elicits guard cell closure, ABA-regulated gene expression, and drought tolerance. Proc Natl Acad Sci USA 110:12132–12137. https://doi.org/10.1073/pnas.1305919110

Otwinowski Z, Minor W (1997) Processing of X-ray diffraction data collected in oscillation mode. Macromol Crystallogr Pt A 276:307–326. https://doi.org/10.1016/S0076-6879(97)76066-X

Park SY et al (2009) Abscisic acid inhibits type 2C protein phosphatases via the PYR/PYL family of START proteins. Science 324:1068–1071. https://doi.org/10.1126/science.1173041

Peterson FC et al (2010) Structural basis for selective activation of ABA receptors. Nat Struct Mol Biol 17:1109–1113. https://doi.org/10.1038/nsmb.1898

Schneider CA, Rasband WS, Eliceiri KW (2012) NIH image to ImageJ: 25 years of image analysis. Nat Methods 9:671–675

Soon FF et al (2012) Molecular mimicry regulates ABA signaling by SnRK2 kinases and PP2C phosphatases. Science 335:85–88. https://doi.org/10.1126/science.1215106

Tischer SV, Wunschel C, Papacek M, Kleigrewe K, Hofmann T, Christmann A, Grill E (2017) Combinatorial interaction network of abscisic acid receptors and coreceptors from Arabidopsis thaliana. Proc Natl Acad Sci USA 114:10280–10285. https://doi.org/10.1073/pnas.1706593114

Vaidya AS et al (2017) A rationally designed agonist defines subfamily IIIA abscisic acid receptors as critical targets for manipulating transpiration. ACS Chem Biol 12:2842–2848. https://doi.org/10.1021/acschembio.7b00650

Weng JK, Ye M, Li B, Noel JP (2016) Co-evolution of hormone metabolism and signaling networks expands plant adaptive plasticity. Cell 166:881–893. https://doi.org/10.1016/j.cell.2016.06.027

Xiong J-L, Dai L-L, Ma N, Zhang C-L (2018) Transcriptome and physiological analyses reveal that AM1 as an ABA-mimicking ligand improves drought resistance in *Brassica napus*. Plant Growth Regul. https://doi.org/10.1007/s10725-018-0374-8

Yuan X, Yin P, Hao Q, Yan C, Wang J, Yan N (2010) Single amino acid alteration between valine and isoleucine determines the distinct pyrabactin selectivity by PYL1 and PYL2. J Biol Chem 285:28953–28958. https://doi.org/10.1074/jbc.m110.160192

Zhang X et al (2012) Complex structures of the abscisic acid receptor PYL3/RCAR13 reveal a unique regulatory mechanism. Structure 20:780–790. https://doi.org/10.1016/j.str.2012.02.019

Zhang XL, Jiang L, Xin Q, Liu Y, Tan JX, Chen ZZ (2015) Structural basis and functions of abscisic acid receptors PYLs. Front Plant Sci 6:88. https://doi.org/10.3389/fpls.2015.00088

Zhao Y, Chow TF, Puckrin RS, Alfred SE, Korir AK, Larive CK, Cutler SR (2007) Chemical genetic interrogation of natural variation uncovers a molecule that is glycoactivated. Nat Chem Biol 3:716–721. https://doi.org/10.1038/nchembio.2007.32